Observation of Through-Hydrogen-Bond $^{2h}J_{HC'}$ in a Perdeuterated Protein

Florence Cordier,* Marco Rogowski,† Stephan Grzesiek,*,† and Ad Bax‡

*Institute of Structural Biology, Forschungszentrum Jülich, 52425 Jülich, Germany; †Institute of Physical Biology, Heinrich-Heine Universität, 40225 Düsseldorf, Germany; and ‡Laboratory of Chemical Physics, National Institute of Diabetes and Digestive and Kidney Diseases, National Institutes of Health, Bethesda, Maryland 20892-0520

It is demonstrated that *J* connectivity between amide protons and hydrogen-bond-accepting carbonyl carbons can be observed in perdeuterated human ubiquitin. A selective pulse scheme is used to detect these small $^{2h}J_{HC'}$ interactions in the presence of the much larger through-covalent-bond $^2J_{HC'}$ and $^3J_{HC'}$ couplings. The ratio of the observed through-H-bond correlation intensity and the $^2J_{HC'}$ connectivity observed in a reference spectrum indicates $^{2h}J_{HC'}$ values of ca. 0.4–0.6 Hz, which are only slightly smaller than the corresponding $^{3h}J_{NC'}$ values. However, for technical reasons, $^{2h}J_{HC'}$ couplings are more difficult to measure than $^{3h}J_{NC'}$. © 1999 Academic Press

A number of recent studies have demonstrated the presence of substantial *J* couplings across hydrogen bonds (H-bonds) in nucleic acids, sugars, proteins, and other molecules (*1–10*). The $^{2h}J_{NN}$ coupling across the H-bond in Watson–Crick base pairs is particularly large (6–7 Hz), and even larger values have been reported for other types of base pairing (*3, 4*). Remarkably, the corresponding $^{1h}J_{HN}$ coupling is considerably smaller (2–4 Hz) and therefore more difficult to detect (*2, 4*). In proteins, ^{15}N–$^{13}C'$ connectivities can be detected across H-bonds (*6–9*), and $^{3h}J_{NC'}$ values closely correlate with H-bond length (*8*). Through-H-bond $^{2h}J_{H-Hg/Cd}$ connectivities between amide protons H-bonded to the sulfur atoms which coordinate the metal (Hg or Cd) in rubredoxin were first observed by Summers and co-workers (*11, 12*), and were found to be as large as 4 Hz. However, despite repeated attempts over the past 10 years, detection of $^{2h}J_{HC'}$ connectivity has remained elusive. Here, we report the first measurement of such *J* couplings in the small globular protein ubiquitin.

In proteins that are uniformly enriched in $^{13}C'$, detection of small, through-hydrogen-bond $^{2h}J_{HC'}$ connectivities is hampered by the presence of the relatively large $^2J_{HC'}$ coupling (ca. 4 Hz), and by the intraresidue $^3J_{HC'}$ coupling, which depends in a Karplus-like manner on the intervening dihedral angle ϕ. When attempting to transfer magnetization from a given amide proton to its H-bonded $^{13}C'$, the much larger $^2J_{HC'}$ and $^3J_{HC'}$ couplings interfere with this process and make it inefficient. However, if band-selective pulses are used, interference from

the $^2J_{HC'}$ and $^3J_{HC'}$ couplings can be avoided, and magnetization transfer can be "focused" on the $^{2h}J_{HC'}$ of interest.

The pulse scheme used in this study is shown in Fig. 1. It is a variation on the regular HMQC experiment (*13*), with two pairs of 180° $^{13}C'/^1H^N$ pulses inserted at the midpoint of the de- and rephasing delays, $2T$. Both $^{13}C'$ and $^1H^N$ 180° pulses are band-selective. The ^1H 180° pulse covers the entire amide region but avoids excitation of the water resonance. This improves water suppression and also avoids homonuclear ^1H–^1H *J* modulation (for protonated or incompletely deuterated proteins). The inversion profile of the 6.6 ms ^{13}C 180° sinc pulse covers approximately a bandwidth of ±50 Hz and leaves ^{13}C spins more than 150 Hz from the ^{13}C carrier essentially unaffected. This ensures that only couplings between amide protons and selected $^{13}C'$ spins can yield antiphase terms of the type $\sin(2\pi JT)$ $H_xC'_z$ at the end of the dephasing period. If nonselective $^{13}C'$ 180° pulses were used, higher order terms would also be generated. Although three-spin terms, $H_yC'_{1z}C'_{2z}$, will be eliminated by the phase cycling, they can dramatically decrease sensitivity of the through-hydrogen-bond correlations of interest. Four-spin terms generally will be small, but are not eliminated by the phase cycle of Fig. 1 and could conceivably give rise to confusing correlations in the 2D spectrum. The use of selective $^{13}C'$ pulses avoids generation of such terms.

If only a single $^{13}C'$, *J*-coupled to a given H^N, is inverted by the shaped $^{13}C'$ pulse, the $H_xC'_z$ term present at time *a* in the pulse scheme of Fig. 1 will be converted into $H_xC'_y$ at the start of the t_1 evolution period, and at the end of t_1 (time point *b*), magnetization is converted back into $\sin(2\pi JT)\cos(\Omega_{C'}t_1)$ $H_xC'_z$, which refocuses to $\sin^2(2\pi JT)\cos(\Omega_{C'}t_1)$ H_y at the start of the detection period. Thus, the H^N–C' intensity will be proportional to $\sin^2(2\pi JT)$. In order to measure the value of $^{2h}J_{HC'}$, the experiment of Fig. 1 is carried out twice: once with the ^{13}C carrier at the position of the preceding $^{13}C'$ (corresponding to $^2J_{HC'}$ connectivity), and once with the $^{13}C'$ shaped pulse applied at the frequency of the carbonyl which is hydrogen bonded to the H^N of interest. As is demonstrated below, in practice, several couplings can be measured simultaneously in this manner, although the method remains time consuming.
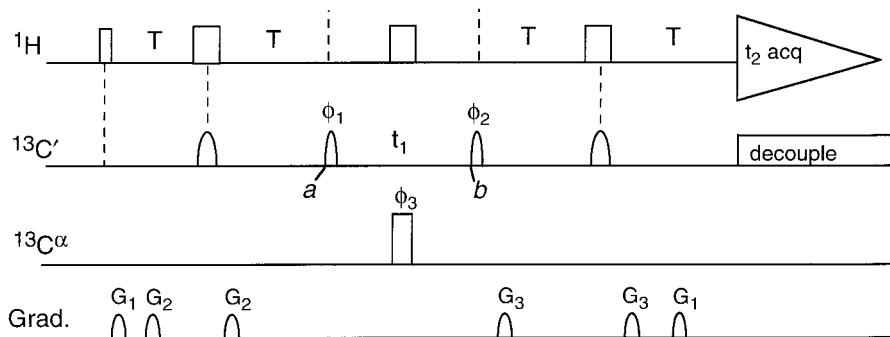
FIG. 1. Pulse scheme of the selective 2D $^1H^N$–$^{13}C'$ HMQC experiment, used to detect through-hydrogen-bond $^{2h}J_{HC'}$ connectivity. Narrow and wide pulses correspond to flip angles of 90° and 180°, respectively. All pulses phases are x, unless specified. $^{13}C'$ pulses have the shape of the center lobe of a (sin x)/x function and durations of 6.6 ms (180°) and 200 μs (90°). ^1H 90° and 180° pulses are rectangular and have durations of 360 (90°) and 320 μs (180°), with the ^1H carrier at 9.2 ppm (for experiments at 600 MHz), such that excitation of the H_2O resonance is minimized and ^1H–^1H J modulation for incompletely deuterated residues is strongly reduced. The $^{13}C^\alpha$ 180° decoupling pulse is rectangular, with a duration of 47 μs, which avoids excitation of the $^{13}C'$ resonances. ^{15}N synchronous composite pulse decoupling (not shown) is used throughout the entire pulse sequence, except for the delay period between scans. The dephasing period, $2T$, was optimized for sensitivity by setting it to 76 ms, slightly shorter than the average amide proton T_2, which was measured to be ca. 90 ms. Phase cycling: $\phi_1 = x, -x$; $\phi_2 = 2(x), 2(-x)$; $\phi_3 = 4(x), 4(-x)$, 4(y), 4($-y$); Receiver = $x,2(-x),x$. Quadrature in the t_1 dimension is obtained by States-TPPI phase incrementation of ϕ_1. Gradients are sine-bell-shaped, with peak amplitudes of 30 G/cm durations; $G_{1,2,3}$ = 0.5, 0.2, and 0.2 ms, and directions z,x, and y, respectively.

The measurement is demonstrated for uniformly $^{15}N/^{13}C/^2H$-labeled ubiquitin, prepared as described by Sass *et al.* (*14*). The sample contained 4 mg of protein in 300 μl 95:5 H_2O/D_2O, pH 6.5, 10 mM phosphate. Experiments were carried out on Bruker DMX-600 and DRX-600 spectrometers, equipped with triple resonance, 3-axis pulsed field gradient probeheads. Spectra were recorded as 128* × 1024* data matrices, with acquisition times of 75 (t_1) and 120 (t_2) ms. For the reference spectrum, aimed at observation of $^2J_{HC'}$ connectivity, eight transients per complex t_1 increment were acquired (total time 33 min); for the spectrum aimed at detection of $^{2h}J_{HC'}$ connectivity, 320 scans per complex t_1 increment were taken (22 h).

Figure 2B shows an example of $^{2h}J_{HC'}$ connectivity for the H-bonds between Val^{70}-H^N and Arg^{42}-C' and between Ile^{44}-H^N and His^{68}-C'. Also visible are two intraresidue $^3J_{HC'}$ connectivities for Val^{70} and Val^{17}, which previously were measured to be 0.83 and 1.46 Hz, respectively (*15*). A strong resonance connecting Leu^{67}-H^N and Thr^{66}-C' corresponds to $^2J_{HC'}$. Figure 2A shows the corresponding reference spectrum, which differs only by a shift in the $^{13}C'$ position from 173.8 to 175.3 ppm and a 40-fold smaller number of scans. Here, only the relatively large $^2J_{HC'}$ couplings (ca. 4.5 Hz) give rise to the observed correlations.

The intensity ratios of the V70/R42 and I44/H68 peaks in Fig. 2B to the respective reference peaks in Fig. 2A, which correspond to $\sin^2(2\pi^{2h}J_{HC'}\ T)/\sin^2(2\pi^2J_{HC'}\ T)$ with $^2J_{HC'}$ = 4.0 Hz (Ile^{44}) and 4.5 Hz (Val^{70}) and $2T$ = 76 ms, yields $^{2h}J_{HC'}$ = 0.59 ± 0.04 Hz for $^{2h}J_{HC'}$(I44/H68) and 0.54 ± 0.04 Hz for $^{2h}J_{HC'}$(V70/R42). Similarly, the Val^{70} intraresidue $^3J_{HC'}$ coupling derived from the intensity ratio corresponds to 1.0 Hz, in fair agreement with the 0.83 ± 0.1 Hz value previously measured with an E.COSY method (*15*).

Using five separate experiments, a total of eight $^{2h}J_{HC'}$ values were measured in ubiquitin. Assuming a linear correlation, $^{2h}J_{HC'} = A\ ^{3h}J_{NC'} + B$, best fitting yields A = 1.08 ± 0.24

and $B = -0.09 \pm 0.14$ Hz, with a correlation coefficient R = 0.94 (Fig. 3). As for large hydrogen bond lengths both types of couplings go to zero, the constant B may be assumed to be zero, yielding $^{2h}J_{HC'}$ = (0.94 ± 0.02) × $^{3h}J_{NC'}$. Although, on average, $^{2h}J_{HC'}$ is only slightly smaller than $^{3h}J_{NC'}$, $^{2h}J_{HC'}$ values are considerably more difficult to measure than $^{3h}J_{NC'}$ interactions. Detection of the $^{2h}J_{HC'}$ connectivities is hampered by the relatively large linewidth of the amide proton, H^N, and also by the presence of two-bond sequential $^2J_{HC'}$ couplings and intra-
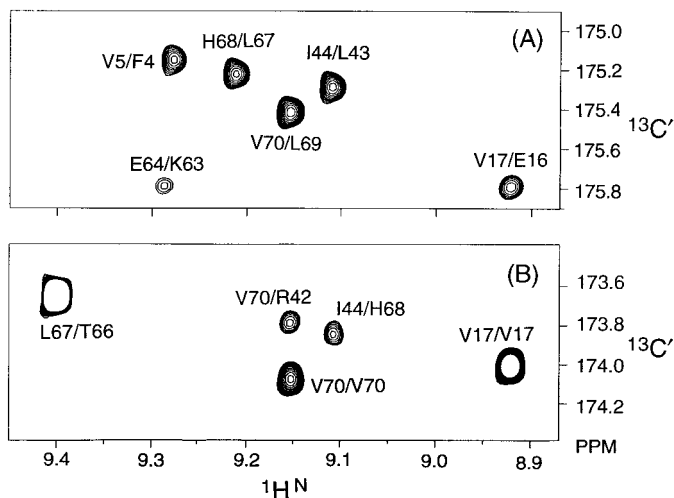
FIG. 2. Small sections of the 600 MHz 2D selective $^1H^N$–$^{13}C'$ HMQC spectra of U–$^2H/^{13}C/^{15}N$ ubiquitin, recorded in H_2O with the pulse scheme of Fig. 1. The $^{13}C'$ carrier was set to 175.3 ppm (A) and 173.8 ppm (B). The reference spectrum (A) was recorded with 8 scans per t_1 increment and shows only sequential $^1H_i^N$–$^{13}C'_{i-1}$ connectivities, through the large (ca. 4.5 Hz) $^2J_{HC'}$ coupling. Spectrum (B), recorded with 320 scans per t_1 increment, shows through-hydrogen-bond J connectivities (V70/R42 and I44/H68), in addition to intraresidue correlations (V70/V70 and V17/V17) and one sequential correlation (L67/T66).
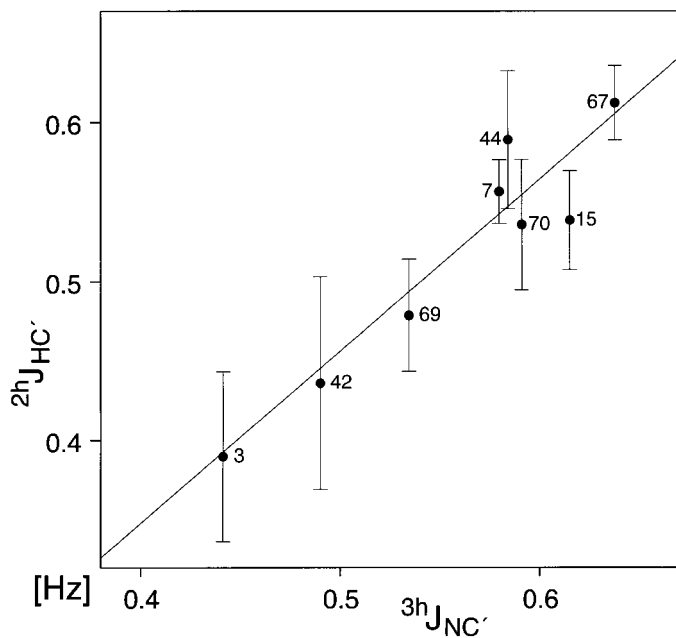
FIG. 3. Plot of $^{2h}J_{HC'}$ values measured in this study versus the corresponding $^{3h}J_{NC'}$ values. Assuming a linear correlation, a best fit yields $^{2h}J_{HC'} = 1.08 \times {}^{3h}J_{NC'} - 0.09$ Hz (solid line), with a correlation coefficient, $R = 0.94$. Error bars correspond to the propagated errors in the measured $^{2h}J_{HC'}$ couplings, assuming that uncertainties in the measured peak heights correspond to the noise level measured in regions of the spectrum without signal. Random errors in $^{3h}J_{NC'}$ are very small (<0.02 Hz).

residue three-bond $^3J_{HC'}$ interactions, which make it necessary to use selective experiments. Deuteration of the nonexchangeable hydrogens, as used in the present study, increases the H^N T_2 values more than twofold, but they remain considerably (25–50%) shorter than the corresponding ^{15}N T_2. Considering the small magnitude of $^{2h}J_{HC'}$, it is not expected that routine detection of such interactions will become widely used for proteins, but similar interactions might be measured more easily in smaller systems, or in cases where very strong hydrogen bonding gives rise to much larger values.

ACKNOWLEDGMENTS

REFERENCES

1. A. J. Dingley and S. Grzesiek, Direct observation of hydrogen bonds in nucleic acid base pairs by internucleotide $^2J_{NN}$ couplings, *J. Am. Chem. Soc.* **120,** 8293–8297 (1998).

2. K. Pervushin, A. Ono, C. Fernandez, T. Szyperski, M. Kainosho, and K. Wüthrich, NMR scalar couplings across Watson–Crick base pair hydrogen bonds in DNA observed by transverse relaxation optimized spectroscopy, *Proc. Natl. Acad. Sci. USA* **95,** 14,147–14,151 (1998).

3. A. Majumdar, A. Kettani, and E. Skripkin, Observation and measurement of internucleotide $^2J_{NN}$ coupling constants between ^{15}N nuclei with widely separated chemical shifts, *J. Biomol. NMR* **14,** 67–70 (1999).

4. A. J. Dingley, J. E. Masse, R. D. Peterson, M. Barfield, J. Feigon, and S. Grzesiek, Internucleotide scalar couplings across hydrogen bonds in Watson–Crick and Hoogsteen base pairs of a DNA triplex, *J. Am. Chem. Soc.* **121,** 6019–6027 (1999).

5. O. Kwon and S. J. Danishefsky, Synthesis of asialo GM1. New insights in the application of sulfonamidoglycosylation in oligosaccharide assembly: Subtle proximity effects in the stereochemical governance of glycosidation, *J. Am. Chem. Soc.* **120,** 1588–1599 (1998).

6. F. Cordier and S. Grzesiek, S. Direct observation of hydrogen bonds in proteins by interresidue $^3J_{NC'}$ scalar couplings, *J. Am. Chem. Soc.* **121,** 1601–1602 (1999).

7. G. Cornilescu, J.-S. Hu, and A. Bax, Identification of the hydrogen bonding network in a protein by scalar couplings, *J. Am. Chem. Soc.* **121,** 2949–2950 (1999).

8. G. Cornilescu, B. E. Ramirez, M. K. Frank, G. M. Clore, A. M. Gronenborn, and A. Bax, Correlation between $^{3h}J_{NC'}$ and hydrogen bond length in proteins, *J. Am. Chem. Soc.* **121,** 6275–6279 (1999).

9. Y.-X. Wang, J. Jacob, F. Cordier, P. Wingfield, S. J. Stahl, S. Lee-Huang, D. A. Torchia, S. Grzesiek, and A. Bax, Measurement of $^{3h}J_{NC'}$ connectivities across hydrogen bonds in a 30 kDa protein, *J. Biomol. NMR* **14,** 181–184 (1999).

10. N. S. Globulev, I. G. Shenderovich, S. N. Smirnov, G. S. Denisov, and H. H. Limbach, Nuclear scalar spin–spin coupling reveals novel properties of low-barrier hydrogen bonds in a polar environment, *Chem. Eur. J.* **5,** 492–497 (1999).

11. P. R. Blake, J.-B. Park, M. W. W. Adams, and M. F. Summers, Novel observation of NH···S(Cys) hydrogen-bond-mediated scalar coupling in ^{113}Cd-substituted rubredoxin from *Pyrococcus furiosus, J. Am. Chem. Soc.* **114,** 4931–4933 (1992).

12. P. R. Blake, M. F. Summers, M. W. W. Adams, J.-B. Park, Z. H. Zhou, and A. Bax, Quantitative measurement of small through-hydrogen-bond and "through-space" *J* couplings in metal-substituted rubredoxin from *Pyrococcus furiosus, J. Biomol. NMR* **2,** 527–533 (1992).

13. A. Bax, R. H. Griffey, and B. L. Hawkins, Correlation of proton and nitrogen-15 chemical shifts by multiple quantum NMR, *J. Magn. Reson.* **55,** 301–315 (1983).

14. J. Sass, F. Cordier, A. Hoffmann, M. Rogowski, A. Cousin, J. G. Omichinski, H. Loewen, and S. Grzesiek, Purple membrane induced alignment of biological macromolecules in the magnetic field, *J. Am. Chem. Soc.* **121,** 2047–2055 (1999).

15. A. C. Wang and A. Bax, Determination of the backbone dihedral angles ϕ in human ubiquitin from reparametrized empirical Karplus equations, *J. Am. Chem. Soc.* **118,** 2483–2494 (1996).